

Antireflective polymer films via roll to roll UV nanoimprint lithography using an AAO mold

Cheng-Hsin Chuang¹ · Deng-Maw Lu¹ · Po-Hsiang Wang¹ · Wen-Yu Lee¹ · Muhammad Omar Shaikh¹

Received: 20 August 2016 / Accepted: 17 January 2017 / Published online: 28 January 2017
© Springer-Verlag Berlin Heidelberg 2017

Abstract Anti-reflection based on the mimicking of moth eye subwavelength structures (SWSs) has several advantages over conventionally used multilayer thin film antireflective coatings like broad angular and spectral responses, polarization insensitivity and improved stability. In this study, we present the low cost fabrication of moth eye based SWSs on flexible polyethylene terephthalate (PET) substrates using roll-to-roll ultraviolet nanoimprint lithography. We have used a novel method to create a roller mold with embedded nanopores that can be used for easy replication of SWSs without demolding issues. Pure aluminum foil was wrapped around an acrylic cylinder ($\varnothing = 90$ mm) and a multistep anodizing and pore widening scheme was employed to create well-ordered and periodic anodized aluminum oxide (AAO) nanopores with different aspect ratios. Optical characterization of the antireflective PET film shows a transmittance over 92%, an increase of 3% as compared to bare PET, while reflectance can be reduced from 5.3 to 0.09% in the range of visible light. It was observed that higher aspect ratio SWSs is more effective in reducing reflections at higher incident angles. Consequently, we have demonstrated an economically feasible method for fabricating large area polymer films that can be used to reduce light reflections which impose severe limitations on the performance of many optoelectronic devices like solar cells, photodetectors and flat display panels.

1 Introduction

An antireflective film helps to reduce reflection when light impinges on an interface between two materials with varying refractive indices and can be utilized in several optoelectronic devices including solar cells (Phillips et al. 2011) and display devices (Song et al. 2010). Traditionally, anti-reflective coatings have utilized the principle of destructive interference of light waves by tuning the thickness and refractive index of the coating film. An anti-reflection coating of a quarter-wave optical thickness is a well-known method for removing reflections of one specific wavelength while multilayer coatings have been used for broadband anti-reflection applications (Raut et al. 2011). Multi-layer thin film coatings have been extensively used for reflectivity modulation in various optical components and consist of layers of nonabsorbent dielectric materials with different refractive indices fabricated by sequential sputtering in a vacuum chamber. The downside to multilayer coatings is the high manufacturing cost and low yield due to several issues such as poor adhesion, limitations in material selection and instability of stacking layers while also posing limitations for large size requirements.

An alternative concept to antireflection which is employed in this study takes inspiration from the nanostructured topography of the corneal lenses found in moth eyes. These cone-like protuberances have size features below the wavelength of visible light and their continuous gradient refractive index renders them almost perfectly antireflective, creating an absolutely lusterless surface (Bernhard 1967; Clapham and Hutley 1973). The progressive bending of light and multiple internal reflections in moth eye resembling sub-wavelength structures (SWSs) results in maximum absorption of the incident radiation

✉ Cheng-Hsin Chuang
chchuang@mail.stust.edu.tw

¹ Department of Mechanical Engineering, Southern Taiwan University of Science and Technology, Tainan 71005, Taiwan

and could reduce reflection in the visible range down to 0.1% (Craighead et al. 1982). To date, various nanolithographic techniques like laser interference lithography and electron beam lithography have been used for patterning etching masks with nanoscale dot arrays on a photoresist layer and SWSs can thus be achieved by wet or dry etching (Han et al. 2011; Jiao et al. 2013). However, the size of the patterned area is limited by the e-beam writing system and laser beam size with high manufacturing costs arising from need of sophisticated facilities. To obtain low-cost nanopatterning, colloidal lithography has been successfully used to fabricate SWS (Askar et al. 2012). However, an ordered self-assembly of nanobeads is difficult to control over a long range, thus hindering the scaling up of this technology. In conclusion, these techniques for fabrication of SWSs are not suitable for commercialization which requires a combination of high-throughput, high-resolution, large-area fabrication and low cost.

A promising technology that has gained widespread attention for fabrication of SWSs is nanoimprint lithography (NIL) where a prefabricated mold is pressed onto a resist coated substrate to replicate an inverse of the mold pattern via direct mechanical deformation. NIL can be broadly categorized based on its two main operation features, namely resist curing (thermal or ultraviolet) and method of imprinting (plate to plate, roll to plate or roll to roll). The major advantage of ultraviolet based NIL (UV-NIL) over thermal or hot embossing methods is the ability to operate at room temperature and elimination of issues arising from thermal expansion between mold, resist and substrate (Vogler et al. 2007). Furthermore, the use of lower viscosity resists in UV-NIL enables imprinting at substantially lower pressures and instantaneous curing using focused UV light, thus making it more suitable for roll to roll NIL (R2R NIL) (Lee et al. 2008). R2R NIL is preferred for industrial scale manufacturing of SWSs as compared to other imprinting techniques as it is a continuous process with improved speed for patterning large area substrates, thus resulting in significantly higher throughput (Ahn and Guo 2008). Furthermore, since it is a roller based imprinting method, mold-substrate separation is easier and requires much less demolding force, thus reducing defect generation.

Several research works reported in literature have utilized a wide variety of modified R2R NIL protocols to pattern SWSs on polymer substrates (Nezuka et al. 2008; Liu et al. 2014). Polymer antireflective films have gained widespread attention owing to their attractive characteristics as opposed to inorganic materials like ease in controlling morphology and porosity, adherence to flexible substrates and large area processing ability. Ahn and Guo (2009) developed a high speed R2R UV-NIL process for large area imprinting of nanostructures on a flexible web using

a fluoropolymer mold and have also performed theoretical analysis to predict residual layer thickness and effects of mold separation direction on the pattern results. Yoshikawa et al. (2013) used high speed R2R UV-NIL for fabrication of high aspect ratio line and space pattern while John et al. (John et al. 2013) have developed a custom designed R2R nanoimprinting system for patterning sub-micron features on polymer substrates. One of the main challenges during R2R-NIL is the fabrication of a low cost and large area mold that is flexible enough to be wrapped around the roller, has sufficient modulus and strength for successful imprinting and possesses a low surface energy for ease in demolding. Anodic aluminum oxide (AAO) provides a simple and inexpensive solution for large area mold fabrication where periodic array of nanopores with hexagonal symmetry can be obtained with relative ease while control of the pore shape, aspect ratio and periodicity can be achieved by simply varying the anodizing voltage and duration. The use of an AAO mold to fabricate SWSs for antireflection purposes is not novel and has been previously investigated. Nanopillars have been obtained by protruding softened polymer materials like polycarbonate (PC) or polymethylmethacrylate (PMMA) into the nanopore array of AAO by casting or hot embossing methods (Hubbard et al. 2012; Choi et al. 2010). Kim et al. fabricated a dense high aspect ratio nanopillar array inspired by gecko's foot hair via UV nano embossing using an AAO mold (Kim et al. 2007). However, these methods are unsuitable for large scale manufacturing of antireflective films and require high cost and time consuming replication protocols. While several research works utilize R2R UV NIL for the fabrication of SWSs, an AAO mold using this process has rarely been reported. In this study, we have developed a high performance antireflective coating with SWSs on a flexible PET substrate using a continuous R2R UV-NIL protocol with an AAO roller mold. The morphology of the AAO mold can be controlled by adjusting anodizing times, thus resulting in the imprinting of SWSs with different aspect ratios.

2 Experimental methods

2.1 Fabrication of AAO based roller mold

To create a roller mold that can be used to imprint moth-eye based SWSs on a PET web during R2R UV-NIL, we used an aluminum foil (99.9995% purity, 290 mm × 210 mm, thickness of 0.25 mm) with impregnated AAO nanopores to wrap around a roller having a diameter of 90 mm as shown in Fig. 1a, b. In order to create a well ordered periodic AAO template, the aluminum foil was subjected to a two-step anodizing process as shown in Fig. 1c. The first long anodization and subsequent etching of the oxide layer results

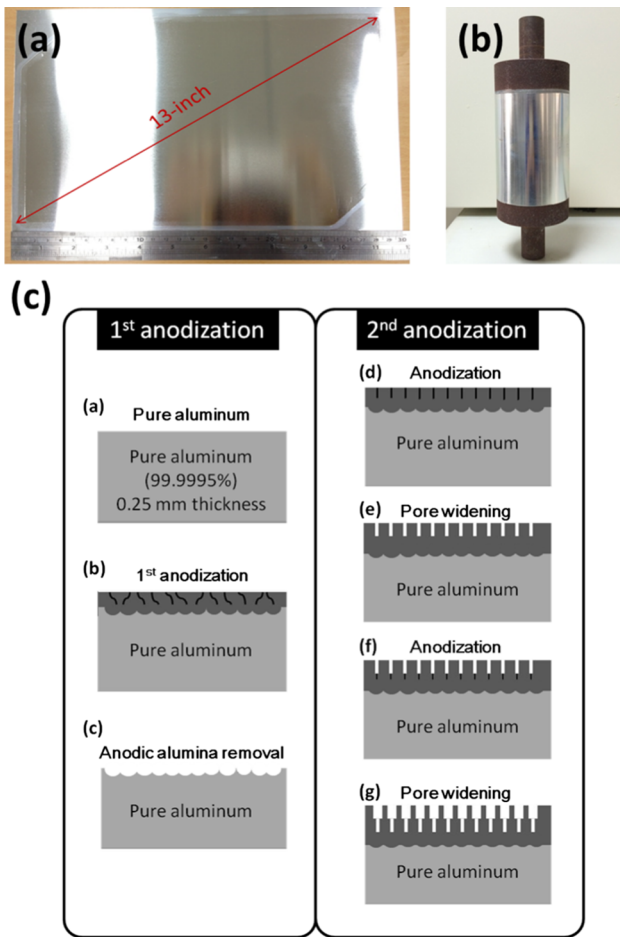


Fig. 1 a Large area AAO mold using high purity aluminum foil. b AAO mold wrapped around roller. c Two step anodizing process for fabrication of AAO mold

in the formation of an ordered array of concaves on the foil surface. During the second step, which consists of multiple short anodization and pore widening cycles, the concaves act as initiation sites for generation of an ordered arrangement of holes from the surface. A constant power supply [N5771A Power Supply, Keysight (Agilent)] was used as a DC power source during the anodization protocol which is carried out in a sealable chamber integrated with a circulating cooling system. The first anodizing step was carried out in 0.3 M oxalic acid solution at 4 °C under a constant voltage of 40 V for 5 h to create an ordered-hole arrangement. Next, the anodic alumina layer is removed during a wet chemical etching step in a phosphoric acid solution (chromic trioxide: phosphoric acid: deionized water = 2 g: 3.5 g: 100 ml) at 70 °C for 30 min. This was followed by the second anodization process which consisted of a five cycle treatment. Each cycle included a short-term anodization and pore-widening process. The conditions for the short-term anodization were identical to that of the first

anodization process while three different time durations of 90, 120 and 150 s were used. The pore widening process used in each cycle was carried out in 5 wt% phosphoric acid solution at 32 °C for 15 min. Finally, the finished AAO template was wrapped around the roller for use in R2R UV-NIL.

2.2 R2R UV-NIL system

We have designed a roll to roll system that can be used for continuous imprinting of moth eye based SWSs on a flexible PET web (100 μm thickness) using UV-NIL as shown in Fig. 2. The fed in PET web is first coated with a UV curable resin followed by a doctor blade mechanism that adjusts the uniformity and thickness of the coated resin. Next, a preheating protocol is used to reduce the viscosity of the resin to enable more efficient penetration into the AAO roller mold cavity. The resist is cured instantaneously via crosslinking during the imprinting step due to the presence of a focused ultraviolet light source (400 W high-pressure mercury lamp with dominant wavelengths of 253 and 365 nm) located close to the imprinting roller, thus resulting in the formation of well-defined SWSs on the PET web. The feeding speed can be varied in the range of 0.5–15 m/min by the active roller located at the end of the R2R process that winds the imprinted PET web while a torsion control system is used to adjust the tension of web. The optimized process parameters used in this study for imprinting of SWSs include a feeding speed of 0.56 m/min and a web tension corresponding to a torque of 0.58 kg cm (after unwinding) and 1.45 kg cm (before winding), while the thickness of the coated resin on the web via the doctor blade mechanism is maintained at 80 μm.

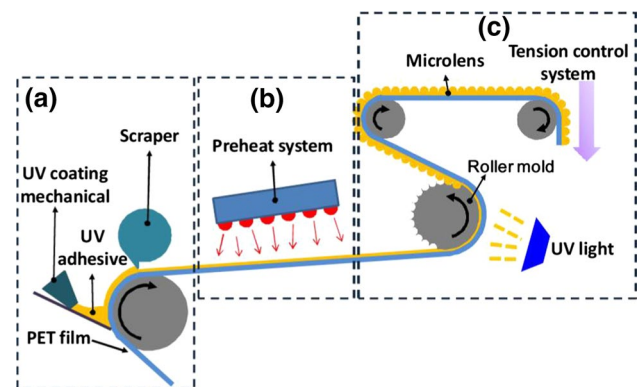


Fig. 2 R2R UV-NIL process used to fabricate SWSs on PET. a Coating the PET web with an 80 μm thick layer of UV resin. b Preheating to reduce viscosity and improve flow properties of UV resin. c Nanoimprinting SWSs on the coated resin using the AAO roller mold followed by curing using UV light irradiation

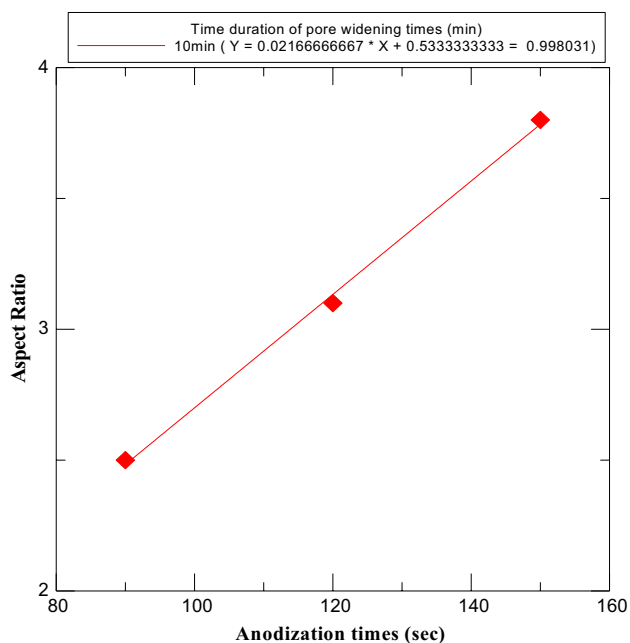


Fig. 3 AAO mold aspect ratio dependence on anodizing time

3 Results and discussion

3.1 Effects of anodizing time on AAO mold

It was observed that increasing the duration of the second anodizing step from 90 s to 120 s and finally to 150 s increased the aspect ratio of the AAO nanopores from 1:2.5 to 1:3.1 to 1:3.8, respectively, as shown in Fig. 3. The effect of the anodizing time on the morphology of the obtained AAO nanopores can be seen in the series of SEM images shown in Fig. 4. The structure of the AAO can be described as a closely packed array of columnar cells where each cell contains an elongated cylindrical nanopore that is normal to the underlying aluminum surface.

Furthermore, the morphology of the nanopores varies from saddle to cone shaped as the anodizing time increases from 90 to 150 s as observed in the schematic illustration shown at the top right of each SEM image obtained via a computer graphics software. Thus we can conclude that increasing the anodizing time increases the nanopore depth and consequently the aspect ratio of the obtained AAO template.

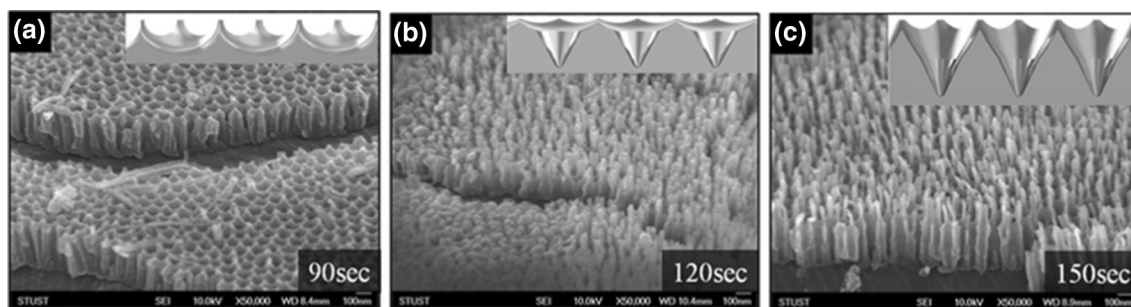


Fig. 4 SEM images of large area AAO mold obtained at different anodizing times of **a** 90 s, **b** 120 s and **c** 150 s while inset shows the schematic cross sectional view of the corresponding AAO nanopores

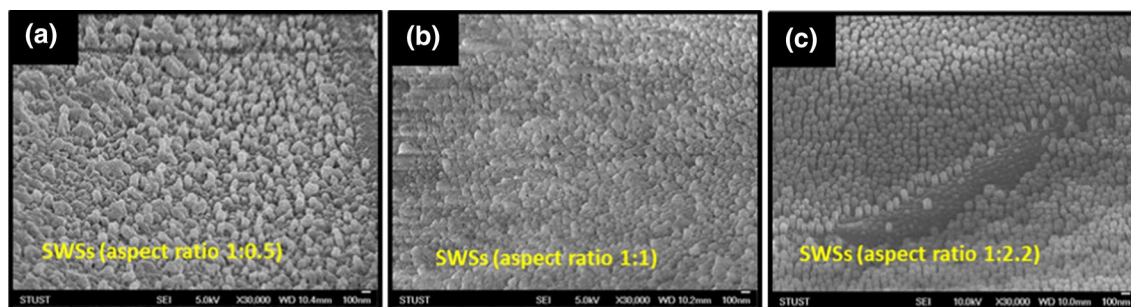


Fig. 5 SEM images of the imprinted SWs on PET having aspect ratios of **a** 1:0.5, **b** 1:1 and **c** 1:2.2 that are obtained using an AAO roller mold containing nanopores with aspect ratios of 1:2.5, 1:3.1 and 1:3.8, respectively

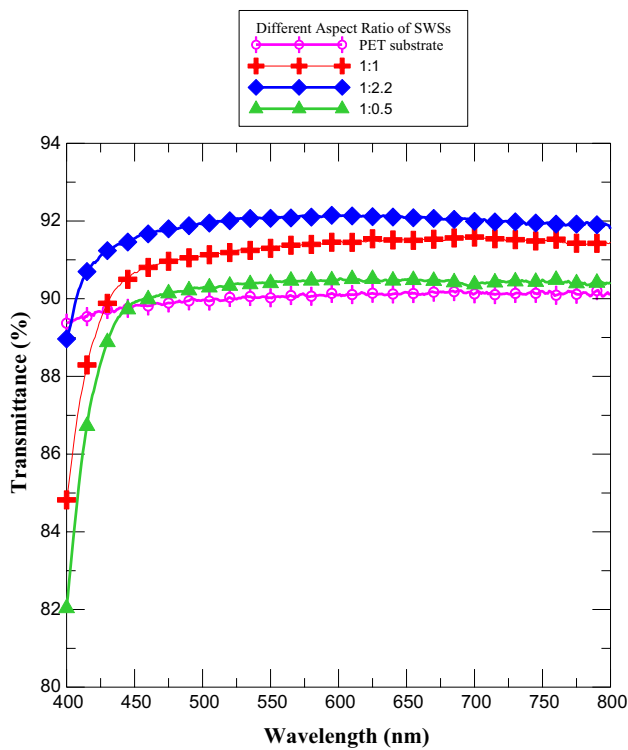


Fig. 6 Transmittance spectra in the visible light region for different aspect ratio SWSs

3.2 Imprinting SWSs using AAO roller mold

We have used AAO molds with varying aspect ratios to imprint the SWSs on the PET web during R2R UV-NIL process as shown in Fig. 5. The three AAO molds with aspect

ratios of 1:2.5, 1:3.1 and 1:3.8 result in imprinted SWSs with aspect ratios of 1:0.5, 1:1 and 1:2.2, respectively, as shown in Fig. 5. Thus the aspect ratio of the obtained SWSs was lower than that of their corresponding AAO molds. The nanopores in the AAO mold are wider on the top and taper towards the bottom. This causes incomplete filling of the nanopores with UV resin during the imprinting step, thus resulting in lower aspect ratio SWSs. Further optimization of process conditions is required to improve duplication of geometry and achieve a replication ratio closer to 1:1.

3.3 Optical properties of PET with imprinted SWSs

The optical measurements of the PET film with imprinted SWSs were obtained using a spectrophotometer (V670, JASCO). It can be seen from Fig. 6 that the transmittance improves for all PET films with imprinted SWSs of different aspect ratios as compared to bare PET for wavelengths in the range of about 450–700 nm. The highest transmittance in this range is observed for SWSs with the largest aspect ratio (1:2.2) with values obtained over 92% which is about 3% higher than bare PET. The observed increase in transmittance for higher aspect ratio SWSs shows good agreement with results obtained in literature using Finite Difference Time Domain (FTD) analysis for moth eye based SWSs (Han and Chang 2014). We have also performed reflectance measurements at incident angles of 5° to 60° as shown in Fig. 7. It was observed that reflectance at an incident angle of 5° can be reduced from over 5% for bare PET to less than 1% for PET with different aspect ratio SWSs over the visible range of about 400–700 nm. The reduction in reflectance was more prominent for higher

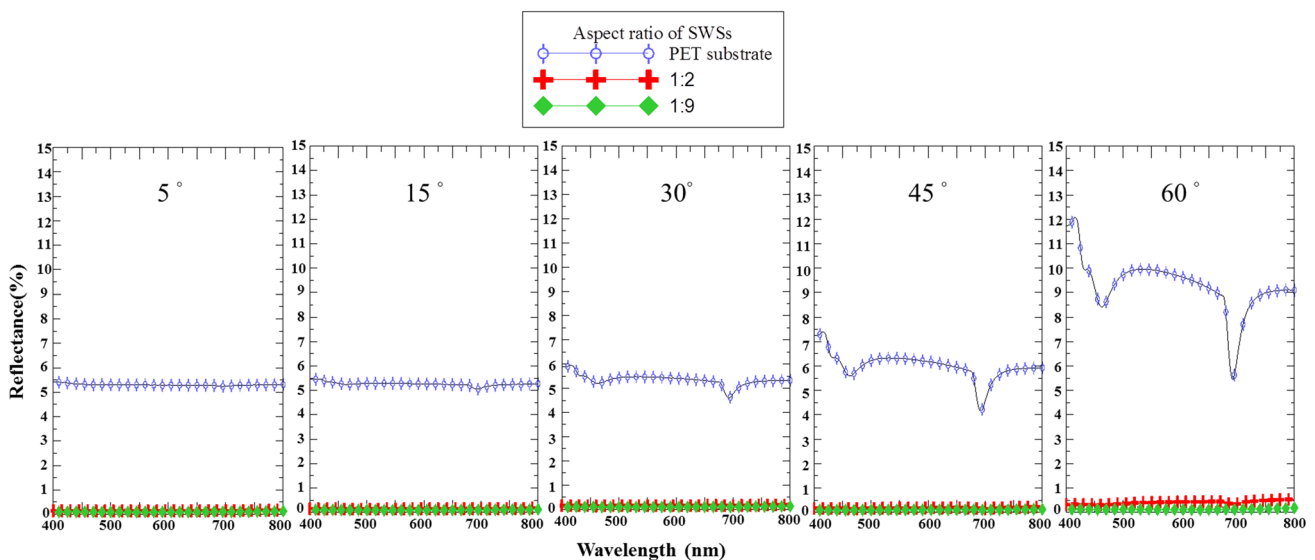


Fig. 7 Reflectance spectra in the visible light region at incident angles of 5° to 60° for different aspect ratio SWSs

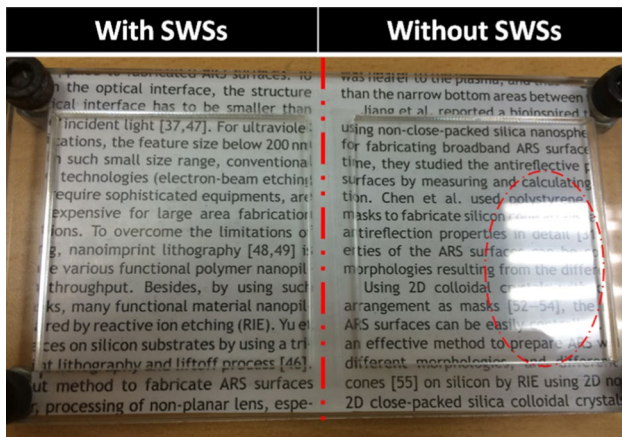


Fig. 8 Antireflective properties of PET films with and without SWSs

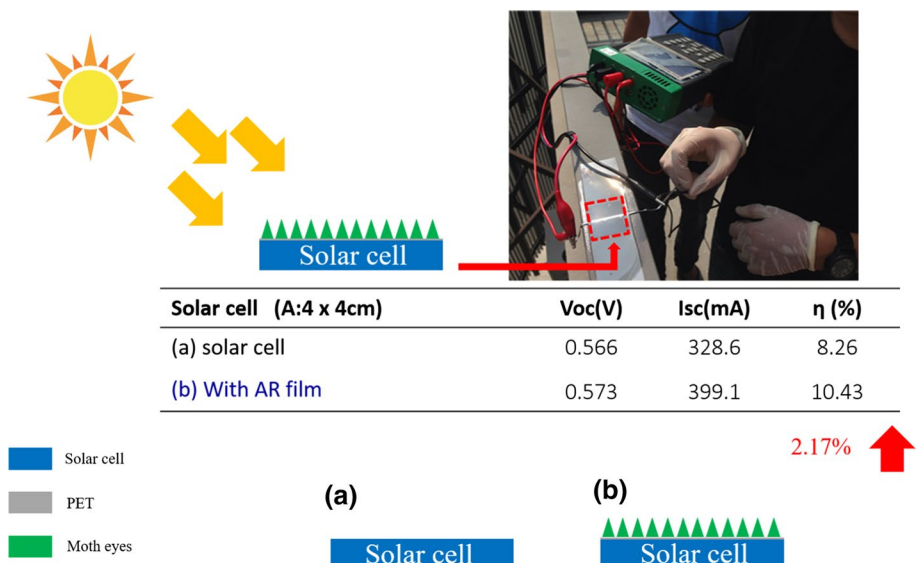
aspect ratio SWSs. Generally, reflectance increases as the angle of incidence increases. However, high aspect ratio SWSs (1:2.2) showed a reflectance of less than 1% even when the incident angle was increased to 30°. Furthermore, the reduction in reflectance increased considerably for SWSs as compared to bare PET as the incident angle increased from 30° to 60°. For example, reflectance was about 8% lower for high aspect ratio SWSs as compared to bare PET at an incident angle of 60°. Thus improved optical properties over a wide range of incident angles can be achieved by using an antireflective PET film imprinted with high aspect ratio SWSs.

3.4 Practical applicability of antireflective PET films

PET films, with and without imprinted SWSs, were placed on top of a printed paper and fixed in position as shown in

Fig. 8. It can be seen that the bare PET film without SWSs causes reflection of the light source present in the room (indicated by the dotted red circle) while no such reflection is observed for the PET film with imprinted SWSs. This shows the viability of using these antireflective films for display applications. The efficiency of solar cells can also be improved by reducing reflections and maximizing the conversion of incident light rays into electricity. Several techniques have been researched to increase the light harvesting efficiency of solar cells which include utilization of light scattering layers, photonic crystals and antireflective coatings (Lee and Lee 2014; Colodrero et al. 2009; Rahman et al. 2015). In particular, biomimetic moth-eye based anti-reflective coatings as developed in this study exhibit ultra-low reflections for omnidirectional light incidences and broadband wavelengths. Furthermore, high throughput manufacturing using a roll to roll process on low cost polymer substrates provides a facile approach for obtaining antireflective coatings on large area solar cells. We demonstrate the viability of achieving improved efficiency by simply coating the surface of a test solar cell with the PET film containing imprinted SWSs. We chose SWSs with an aspect ratio of 1:2.2 for which optimal optical performance (transmittance and reflectance) can be achieved as shown in Figs. 6 and 7. The performance of the solar cell was compared with and without the film coating and tests were performed outdoors under direct solar illumination. The antireflective film coating resulted in improved solar cell performance with a higher open circuit voltage (V_{oc}) and short circuit current (I_{sc}) and consequently an increase in the observed efficiency from 8.26 to 10.43% as shown in Fig. 9. Furthermore, since the SWSs can minimize reflections over a wide range of incident angles, improved photoelectric conversion efficiency can be attained without relying on a tracking system. Consequently,

Fig. 9 Comparison of photoelectric conversion efficiency of solar cell **a** without an antireflective film and **b** with an antireflective film



we have demonstrated the practical applicability of polymer antireflection films with moth eye based SWSs fabricated via high throughput and low cost R2R UV-NIL.

4 Conclusion

We have successfully fabricated large area broadband antireflective films by imprinting SWSs on flexible PET substrates via a custom designed R2R UV-NIL process. We have developed a novel roller mold based on a periodically patterned AAO nanoporous structure and the morphology of the obtained AAO mold can be varied by controlling the anodizing duration, thus resulting in SWSs with varying aspect ratios. The highest transmittance (over 92%) across the visible light region was observed for SWSs with the highest aspect ratio of 1:2.2, with significantly reduced reflectance as compared to bare PET, especially at higher incident angles. The developed roll to roll process is a promising, cost effective and high throughput method for the industrial production of moth eye nanostructure arrays for antireflective coatings.

Acknowledgements The authors would like to thank the Southern Taiwan University of Science and Technology Office of Paradigm Technology University for financially supporting this research under Contract No. I000100P088.

References

- Ahn SH, Guo LJ (2008) High-speed roll-to-roll nanoimprint lithography on flexible plastic substrates. *Adv Mater* 20:2044–2049
- Ahn SH, Guo LJ (2009) High speed roll-to-roll nanoimprint lithography on flexible substrate and mold-separation analysis. *Proc SPIE* 7205:72050U-1–72050U-10
- Askar K, Phillips BM, Dou X, Lopez J, Smith C, Jiang B, Jiang P (2012) Self-assembled nanoparticle antiglare coatings. *Opt Lett* 37:4380–4382
- Bernhard CG (1967) Structural and functional adaptation in a visual system. *Endeavour* 26:79–84
- Choi K, Park SH, Song YM, Lee YT, Hwangbo CK, Yang H, Lee HS (2010) Nano-tailoring the surface structure for the monolithic high-performance antireflection polymer film. *Adv Mater* 22:3713–3718
- Clapham PB, Hutley MC (1973) Reduction of lens reflexion by the ‘moth eye’ principle. *Nature* 244:281–282
- Colodrero S, Mihi A, Häggman L, Ocaña M, Boschloo G, Hagfeldt A, Míguez H (2009) Porous one-dimensional photonic crystals improve the power-conversion efficiency of dye-sensitized solar cells. *Adv Mater* 21:764
- Craighead HG, Howard RE, Sweeney JE, Tenant DM (1982) Textured surfaces: optical storage and other applications. *J Vac Sci Technol* 20:316–319
- Han K, Chang CH (2014) Numerical modeling of sub-wavelength anti-reflective structures for solar module applications. *Nanomaterials* 4:87–128
- Han KS, Shin JH, Yoon WY, Lee H (2011) Enhanced performance of solar cells with anti-reflection layer fabricated by nano-imprint lithography. *Sol Energy Mater Sol Cells* 95:288–291
- Hubbard G, Nasir ME, Shields P, Bowen CR, Satka A, Parsons KP, Holmes NH, Allsopp DWE (2012) Angle dependent optical properties of polymer films with a biomimetic anti-reflecting surface replicated from cylindrical and tapered nanoporous alumina. *Nanotechnology* 23:155302
- Jiao F, Huang Q, Ren W, Zhou W, Qi F, Zheng Y, Xie J (2013) Enhanced performance for solar cells with moth-eye structure fabricated by UV nanoimprint lithography. *Microelectron Eng* 103:126–130
- John J, Tang YY, Rothstein JP, Watkins JJ, Carter KR (2013) Large area, continuous roll-to-roll nanoimprinting with PFPE composite molds. *Nanotechnology* 24:505307-1–505307-9
- Kim DS, Lee HS, Lee J, Kim S, Lee KH, Moon W, Kwon TH (2007) Replication of high-aspect-ratio nanopillar array for biomimetic gecko foot-hair prototype by UV nano embossing with anodic aluminum oxide mold. *Microsyst Technol* 13:601–606
- Lee J, Lee M (2014) Diffraction-grating-embedded dye-sensitized solar cells with good light harvesting. *Adv Energy Mater* 4:1300978
- Lee J, Park S, Choi K, Kim G (2008) Nano-scale patterning using the roll typed UV-nanoimprint lithography tool. *Microelectron Eng* 85:861–865
- Liu CH, Niu PL, Sung CK (2014) Integrating anti-reflection and superhydrophobicity of moth-eye-like surface morphology on a large-area flexible substrate. *J Phys D Appl Phys* 47:015401-1–015401-5
- Nezuka O, Yao DG, Kim BH (2008) Replication of microstructures by roll-to-roll UV-curing embossing. *Polym Plast Technol* 47:865–873
- Phillips BM, Jiang P, Jiang B (2011) Biomimetic broadband antireflection gratings on solar-grade multicrystalline silicon wafers. *Appl Phys Lett* 99:191103-1–191103-3
- Rahman A, Ashraf A, Xin H, Tong X, Sutter P, Eisaman MD, Black CT (2015) Sub-50-nm self-assembled nanotextures for enhanced broadband antireflection in silicon solar cells. *Nat Commun* 6:5963
- Raut HK, Ganesh VA, Nair AS, Ramakrishna S (2011) Antireflective coatings: a critical, in-depth review. *Energy Environ Sci* 4:3779–3804
- Song YM, Choi ES, Park GC, Park CY, Jang SJ, Lee YT (2010) Disordered antireflective nanostructures on GaN-based light-emitting diodes using Ag nanoparticles for improved light extraction efficiency. *Appl Phys Lett* 97:093110–093113
- Vogler M, Wiedenberger S, Mühlberger M, Bergmair I, Glinsner T, Schmidt H, Kley EB, Grützner G (2007) Development of a novel, low-viscosity UV-curable polymer system for UV-nanoimprint lithography. *Microelectron Eng* 84:984–988
- Yoshikawa H, Taniguchi J, Tazaki G, Zento T (2013) Fabrication of high-aspect-ratio pattern via high throughput roll-to-roll ultraviolet nanoimprint lithography. *Microelectron Eng* 112:273–332